

# We are IntechOpen, the world's leading publisher of Open Access books Built by scientists, for scientists

4,800

Open access books available

122,000

International authors and editors

135M

Downloads

Our authors are among the

154

Countries delivered to

TOP 1%

most cited scientists

12.2%

Contributors from top 500 universities



WEB OF SCIENCE™

Selection of our books indexed in the Book Citation Index  
in Web of Science™ Core Collection (BKCI)

Interested in publishing with us?  
Contact [book.department@intechopen.com](mailto:book.department@intechopen.com)

Numbers displayed above are based on latest data collected.

For more information visit [www.intechopen.com](http://www.intechopen.com)



# Finite Element modelling of Elastic-Plastic Contact of Rough Surfaces

Jamil Abdo, M. Danish Haneef and Abdullah M. Al-Shabibi  
*Sultan Qaboos University  
Oman*

## 1. Introduction

An improved mathematical elastic-plastic model for the contact of rough surfaces that is based on an accurate finite elements solution of a deformable single asperity and a rigid flat surface is developed to provide dimensionless expressions for the contact area and contact load. This model differs from the existing models, in that it accounts for the level of interference beyond expected failure. The finite element solution is used to define the limits at which failure occurs. The derivation of the contact model is facilitated through the definition of the ultimate-stress asperities that are assumed to be embedded at a critical depth within the actual surface asperities. This model considers a realistic picture of elastic-plastic deformation where elastic, plastic and failure behaviors can occur simultaneously for an asperity. Subsequent comparison of the results for estimating contact area and load using the present model and the earlier methods shows identical results for pure elastic contacts with plasticity index values at about 0.5 but substantial difference for the net elastic-plastic contacts having plasticity index values above 0.8. When plasticity index reaches 6 and beyond the three models predicts similar total contact area and load values and that the contact is purely plastic.

## 2. Background

The role of surface roughness in contact mechanics is relevant to processes ranging from adhesion to friction, wear and lubrication<sup>1</sup>. It also promises to have a deep impact on applied science, including coatings technology and design of micro electro-mechanical systems. Despite the considerable results achieved by indentation experiments<sup>4</sup>, particularly in the measurement of bulk hardness on small scales, the contact behavior of realistic surfaces, showing random multi-scale roughness, remains largely unknown. In many engineering applications, frictional contact occurs between machine parts and the characterization of contact behavior becomes an important subject in solving tribological problems such as friction induced vibration (Brockley, 1970; Ibrahim & Rivin, Tzou et al.,1998; Abdo, 2006), wear (Mulhearn & Samuels, 1962; Samuels, 1978; Archard, 1953; Halling et al.,1975; Abdo & Yahmadi, 2004), issues related to mechanical sealing, performance and life of machine elements, and thermal to name few. The pioneering work

of Greenwood and Williamson (Greenwood & Williamson, 1966) (GW model) has been utilized by many researchers (Greenwood & Tripp, 1970; Chang et al., 1987; Zhao et al., 2000; Abdo & Farhang, 2005) as a basic for further extension to obtain contact models for general or specific contact problems for mainly elastic contact. On the other hand, the work of Pullan and Williamson (Pullen & Williamson, 1972) utilized as a basic model for pure plastic contact. In an attempt to bridge the gap between the pure elastic and pure plastic contact, Chang et al. (CEB model) developed a wide intermediate range of interest where elastic-plastic contact triumph. The existing probabilistic models of contact may be viewed with respect to the premise of elastic and plastic contact. The elastic models primarily rely on the Hertz theory of contact between two elastic bodies (Greenwood & Williamson, 1966; Greenwood & Tripp, 1967; Greenwood & Tripp, 1970; Hisakado, 1974; Bush et al., 1975; McCool, 1986). These models differ in their assumptions related to surface and asperity geometry and material properties. These extensions have included, for instance, the inclusion of the surface curvature effects (Greenwood & Tripp, 1967), allowance for non-uniform curvature of asperity summits (Hisakado, 1974) and presumption of average elliptic paraboloidal representation of asperity (Bush et al., 1975). Whereas the elastic and plastic models are seen to be advantageous for extreme cases of loading, in a large number of engineering applications, contact loads may fall within ranges that do not warrant adequate representation by either elastic or plastic model. This fact has led researchers to consider what is referred to as elastic-plastic models (Chang et al., 1987; Ishigaki et al., 1987). The Zhao model [Zhao et al., 2000] suggests that the contact interference at the inception of fully plastic deformation would be at least 54 times that of the initiating yielding. However, the exact inception of fully plastic deformation was still not given. All of the initial models do not provide a solution due to the basic problem of lacking accuracy in the elastic-plastic contact regime. Such accurate solution calls for the use of a Finite Element Method (FEM)

### **3. General Approach to solve contact problems by FEM**

Due to the complex contact mechanics the scientific community has become more and more interested in using the finite element method to solve contact problems. Analytical solutions for the elastic-plastic asperities interaction are limited and constrained by a number of assumptions and approximations. Finite element analysis is a powerful tool when analytical solutions are difficult to obtain. The idea of finite element is based on the discretization of the continuous domain or geometry into sub-domains or elements. An approximate solution is then sought for each element and integrated with solution of the other elements. The accuracy of the approximated solution depends solely on the number of elements used. To determine the appropriate number of elements, a series of run needs to be performed where the convergence of the finite element solution is monitored. Finite element analysis has been extensively used to study the elastic-plastic interaction between asperities and rigid flat surface. (Kogut & Etsion, 2002) presented a finite element solution of a single asperity contact. Their model have provided more accurate results for the contact parameters such as separation, contact area and contact pressure as functions of the plasticity index and contact load. (Jackson & Green, 2004) presented a finite element study of an elastic-plastic hemisphere in contact with a rigid flat surface. In order to improve the efficiency of computation, Jackson and Green (2005) developed an axisymmetric 2-D model (Fig.1). They used commercially available ANSYS software to for the analysis and produced more

refined results than Kogut & Etsion (2002). The contact region was meshed by 100 contact elements. The meshed contact area also controlled to ensure that at least 30 contact elements are in contact for each applied interference. These are in essence very stiff springs attached between surface nodes and they activate only when penetration onset into the rigid flat is detected.

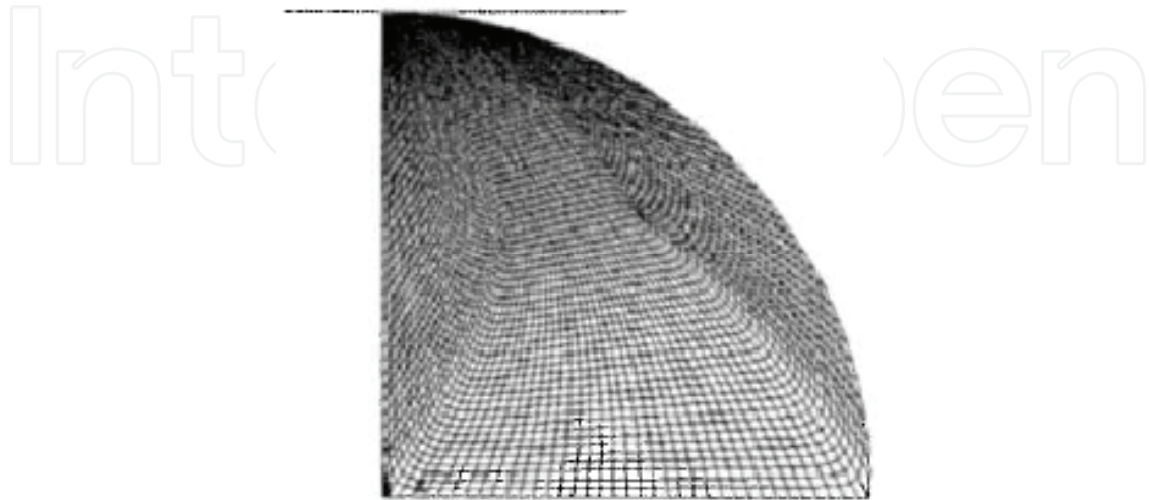


Fig. 1. Finite element mesh of a sphere generated by ANSYS

They found that the fully plastic average contact pressure is not constant and varies with the deformed contact geometry. They also extended the range of  $\omega/\omega_c$  beyond the 110 considered by Kogut and Etsion. (Eid & Adams, 2007) used finite element analysis to study the interaction of two-hemispherical asperities with a flat rigid surface. In their study they have considered asperities of different heights and separations. They presented dimensionless results for the contact force and contact area versus interference. Generally though, the differences are small enough that the FEM solutions practically confirms to the Hertzian solution at interferences below critical (and even slightly above). In this presented work the finite element method was used to solve the elastic-plastic contact of a single asperity. The contact problem and the elasto-plastic material property make the analysis highly nonlinear and difficult to converge. An iterative scheme is used to solve for the solution, and many load steps are used to enhance solution convergence. Initially, a small interference is set of the total interference and then it is incremented after the load step converges. ANSYS internally controls the load stepping to obtain a converged solution by using the bisection method. This continues until a converged solution is found for the desired interference. This work presents an elastic-plastic contact model of flat on rough surface. It is based on the work developed by (Abdo & Farhang , 2005). A fictitious ultimate stress asperity is introduced to facilitate the derivation of the contact model. The finite element method is utilized to define the limit of the expected failure.

#### 4. Overview of the Contact Model

The contact between smooth and rough surface is considered. The contact model is based on the presumption that a surface can, in effect, be represented by a distribution of asperities (Fig. 1). As two surfaces are brought into contact, the macroscopic contact characteristic in

question is a cumulative effect of localized interactions of the smooth surface and the asperities on the rough surface. This approach has required the statistical formulation of a surface and statistical summation of microscopic contact effects to obtain probabilistic macroscopic expectation of the contact characteristic (contact area, load, and stiffness). Many of the contact models predict extreme situations; contact is purely elastic or purely plastic.

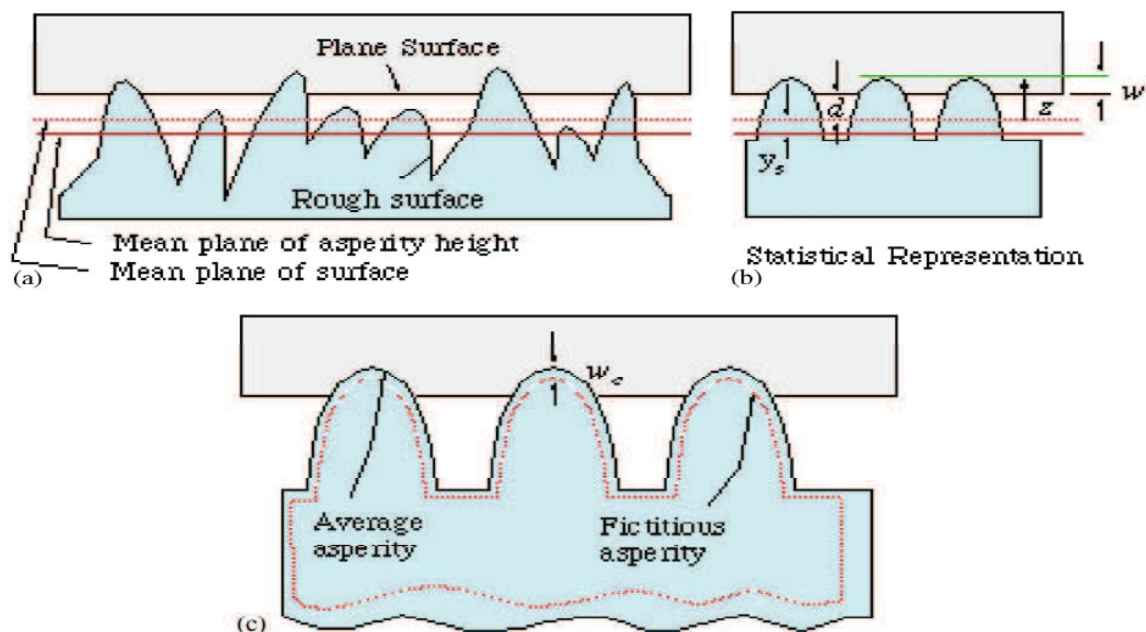


Fig. 2. Contact between a flat and a rough surface

However, the contact is better described, for moderate load ranges, when it includes both elastic and plastic contacts. The proposed model approximates the behavior of the intermediate load ranges, which is referred to as elastic-plastic contact model. In the derivation of the equations the contact between one asperity on a rough surface and a plane is considered. The behavior of the asperity is initially elastic. As the load is increased the elastic behavior continues to describe the deformation until a critical interference is reached. At this critical load and beyond, the asperity deforms as a purely plastic body. Hence, for every asperity there are two types of interactions. The first is the elastic contact between the plane and the surface asperity. If the interference ( $w$ ) exceeds the critical interference ( $w_c$ ), then the interaction also includes plastic contact. The shaded volume representing the interference of the plastic asperities and the plane contribute to the plastic portion of contact whereas the remaining volume of interference contributes to the elastic contact (Fig. 2).

## 5. The Mathematical Model

In a recent pioneering work by Abdo and Farhang (AF model) presented the plastic asperity concept for modeling the elastic-plastic contact of rough surfaces. The salient feature of their approach is outlined here in brief in order to set a scene for the present analysis. Considering the contact between one single asperity on rough surface and a rigid plane, the behavior of the asperity is initially elastic. As the load is increased the elastic behavior continues to describe the deformation until a critical interference is reached. At this critical load and beyond, the asperity deforms as a purely plastic body. Hence for every asperity

there are two types of interactions. The first is the elastic contact between the plane and the asperity. If the interference ( $\omega$ ) exceeds the critical interference ( $\omega_c$ ), then the interaction also includes plastic contact. Abdo and Farhang considered elastic-plastic contact through the introduction of a fictitious asperity that can only deform plastically. The characteristics of contact (area, or load)  $Q$ , in AF model is defined as

$$Q = Q_{e1} - Q_{e2} + Q_{p2} \quad (1)$$

Where ( $Q_{e1}$ ) is the characteristic of contact corresponding to the contribution due to the elastic interference between the plane and surface asperity, ( $Q_{e2}$ ) is the characteristic of contact corresponds to the contribution due to the elastic interference between the plane and plastic asperity and must be subtracted from ( $Q_{e1}$ ) to obtain the net elastic contribution. Next the contribution from plastic interaction due to the plastic interference of the plane and plastic asperity ( $Q_{p2}$ ) must be added to the result to obtain the net elastic-plastic characteristics of contact.

In this work, the elastic-plastic contact model (AF model) of rough surfaces is developed further to account for the level of interference beyond which failure is expected. That is if the interference in AF model is increased further until it equals or exceeds the critical interference corresponds to the ultimate stress of the material ( $\omega_u$ ) at which failure to occur, then the interaction results in failure of the surface asperity and the interference volume will be separated from the asperity.

To account for the level of interference beyond expected failure, Fig. 3 that describes schematically the geometry of the three types of interactions of contacting of rough surfaces is introduced. Therefore, the characteristics of contact,  $Q$ , may be obtained by appropriately accounting for the aforementioned interactions. That is

$$Q = Q_{e1} - Q_{e2} + Q_{p2} - Q_{p3} \quad (2)$$

As it is shown in Fig. 3, the plastic portion of the interference may also include the interference with the ultimate-stress asperity ( $Q_{p3}$ ), which is to be subtracted from ( $Q_{p2}$ ) to give the net plastic interference. The critical interferences ( $\omega_c$ ) and ( $\omega_u$ ) in Fig. 3 are used to define the limits of the plastic and ultimate-stress asperities, respectively. The surfaces of the plastic and the ultimate-stress asperities are obtained by displacement of every point on the physical asperity by ( $\omega_c$ ) and ( $\omega_u$ ) along the direction normal to the original surface asperity. Using mathematical mapping of a point on the physical asperity to a corresponding point on the ultimate-stress asperity and similar to the derivation of the summit radius of curvature of the plastic asperity ( $R_p$ ) in (Abdo & Farhang, 2005) an expression for the summit radius of curvature for the ultimate-stress asperity ( $R_u$ ) can be presented as

$$R_u = R - \omega_u \quad (3)$$

where  $R$  is the radius of curvature for the original surface asperity and ( $R_p$ ) is derived by Abdo & Farhang as (See appendix A)

$$R_p = R - \omega_p \quad (4)$$

The ultimate-stress asperity is assumed to be embedded at a critical depth of ( $\omega_u$ ) within the actual surface asperities. In **Fig. 3**, the shaded volume representing the interference of the plastic asperities and the plane contribute to the plastic portion of contact. The interference beyond this plastic portion of contact will be separated from the asperity. The model consider the interaction of a rough surface covered with a number of asperities that have a spherical shape at their summits with uniform asperity radius of curvature,  $R$ , asperity height,  $z$ , and separation of the surfaces,  $d$ , and a nominally flat surface.  $z$  and  $d$  are measured from the reference plane define by the mean of the original surface heights.  $h$  represents the separation based on surface heights and the standard deviations  $\sigma_s$  and  $\sigma$  correspond to the asperity and surface height, respectively. The difference between  $h$  and  $d$  is denoted as  $y_s$ .

The expected number of asperities in contact is

$$N_c = N \int_{d^*}^{\infty} \phi^*(z^*) dz^* \quad (5)$$

where the total number of asperities,  $N$ , the density of asperities,  $\eta$ , and the nominal area are related according to

$$N = \eta A_n \quad (6)$$

where all length dimensions are normalized by  $\sigma$  and the dimensionless values are denoted by  $*$  and the dimensionless asperity height probability density function is

$$\phi^*(z^*) = (2\pi)^{-0.5} (\sigma/\sigma_s) \exp\left[-0.5(\sigma/\sigma_s)^2 (z^*)^2\right] \quad (7)$$

For this type of contact, the dimensionless interference is define as

$$\omega^* = z^* - d^* \quad (8)$$

The contact of rough surfaces can be modeled by a flat and a smooth surface in contact with a rough surface. The assumptions are along with the ones given by GW model and CEB model. Since the plastic asperity only deform plastically and by imposing the conversation of volume, Abdo and Farhang derived the equations describing the elastic contact area  $A_e$ , the elastic contact load  $P_e$ , the plastic contact area  $A_p$  and the plastic contact pressure  $P_p$  as:

$$A_e = \pi R \omega \quad (9)$$

$$P_e = \frac{4}{3} ER^{1/2} \omega^{3/2} \quad (10)$$

$$A_p = 2\pi R_p \omega \quad (11)$$

$$P_p = 2\pi KHR_p \omega \quad (12)$$

The limit of elastic interference  $\omega_c$  at the inception of elastic-plastic is defined in GW model and AF model:

$$\omega_c = \left( \frac{\pi KH}{2E} \right)^2 R \quad (13)$$

where  $H$  is the hardness of the softer material of the contacting surfaces and  $K$ , the hardness coefficient, is related to the Poisson ratio of the softer material by (Lin & Lin, 2005)

$$K = 0.4645 + 0.3141\nu + 0.1943\nu^2 \quad (14)$$

$E$  is the Hertz elastic modulus and given by

$$\frac{1}{E} = \frac{1-\nu_1^2}{E_1} + \frac{1-\nu_2^2}{E_2} \quad (15)$$

$E_1$ ,  $E_2$  and  $\nu_1$ ,  $\nu_2$  are Young's moduli and Poisson's ratios of the contacting surfaces, respectively.

From the end of the fully elastic deformation to the inception of fully plastic deformation, the contact of the two surfaces goes through an elastic-plastic deformation. At the inception of fully plastic, the maximum contact pressure  $P_{\max}$  of an asperity changes from  $KH$  to  $H$ . Therefore, the plastic contact pressure at the inception of fully plastic deformation can be written as:

$$P_p = 2\pi HR_p \omega \quad (16)$$

## 6. The Finite-Element Model

While an accurate measurement of  $\omega_u$  is not easy to obtain, the minimum value at which failure is expected to occur may be estimated based on a finite element analysis. Using a finite element method (Kogut & Estion, 2002) found that the entire elastic-plastic contact regime of a single asperity extends over the range  $1 \leq \omega/\omega_c < 110$ , with a transition at  $\omega/\omega_c = 6$  that divides it into sub-regions. In the present work, an axisymmetric two-dimensional finite element model was constructed to model and solve the asperity contact problem, using commercial software ANSYS 8.1. The asperity was modeled by a quarter of circle. The Von Mises yielding criterion was used to detect the transition from elastic to



elastic-plastic deformation. The rigid flat was modeled by a line and the material of the sphere was assumed elastic-perfectly plastic with identical behavior in tension and compression. The input parameters were normalized with respect to  $\omega_c$ . The normalization of the output parameters was done with respect to the yield strength  $Y$  of the sphere material. As in Kogut and Etsion (2002) the validity of this normalization was tested by solving the problem for different material properties  $100 < E/Y < 1000$ ,  $\nu = 0.3$  and sphere radii ( $0.1\text{mm} < R < 10\text{mm}$ ). The dimensionless results of  $P/P_c$ ,  $A/A_c$  and  $p/Y$  versus the dimensionless interference,  $\omega/\omega_c$  were always the same regardless of the selection of material properties and sphere radius.

The mesh was composed of 1792 eight-node quadrilateral axisymmetric elements comprising a total of 5537 nodes. For a good representation of the contact geometry, higher order elements are selected to better fit the curvature of the sphere. A zero displacement in all directions is specified for the nodes at the bottom and symmetry boundary conditions are applied for the nodes along the centerline. The finite element model was verified with results obtained from measurements and simulations of Kogut and Etsion.

To accurately compare to their work, the region was divided into two mesh densities. Zone I within a  $0.1R$  distance from the sphere tip has a higher mesh density consisting of 43% of the nodes and 44% of elements, to better capture the high stress concentration and achieve an accurate discrimination for detection of the contact area radius. In this region the mesh size was  $0.001a_c$  where  $a_c = (R\omega_c)^{1/2}$ . Zone II outside the  $0.1R$  distance, had a coarser mesh compared to that of Zone I. The model also contained a single 2-D target element laying on the flat surface and 32 two dimensional surface-to-surface contact elements on the sphere surface in Zone I. A series of runs were conducted and for each run an incremental displacement was applied to the rigid body. The contact forces are obtained from the nodal forces of the active contact elements. The length of the contact zone is determined from the number of the active contact elements. For each run the Von Mises stress is checked to determine the extension of the plastic zone. Fig. 4 shows the evolution of plastic region when  $\omega/\omega_c < 11$ . Up to  $\omega/\omega_c = 6$ , the plastic region is completely surrounded by elastic material. At  $\omega/\omega_c = 6$ , the plastic region first reaches the sphere surface at a radius of about  $3a_c$ . At this point an elastic core remains locked between the plastic region and the sphere surface. Therefore, it is anticipated that this critical interference ( $\omega_u$ ) corresponds to the interaction between the flat surface and the ultimate-stress asperity. The interference beyond this critical interference will be separated from the asperity.

Utilizing Eqn. (2), the derivation presented in the previous section and the dimensionless length definition one can obtain the dimensionless contact area between rough surfaces:

$$A(d) = A_{e1} - A_{e2} + A_{p2} - A_{p3} \quad (17)$$

where,

$$A_{e1}(d) = \pi\beta \int_d^\infty \omega \phi(z) dz \quad (18)$$

$$A_{e2}^*(d) = \pi\beta_p \int_{d+\omega_c}^{\infty} \omega_p^* \phi^*(z) dz \quad (19)$$

$$A_{p2}^*(d) = 2\pi\beta_p \int_{d+\omega_c}^{\infty} \omega_p^* \phi^*(z) dz \quad (20)$$

$$A_{p3}^*(d) = 2\pi\beta_u \int_{d+\omega_u}^{\infty} \omega_{pu}^* \phi^*(z) dz \quad (21)$$

where  $\beta, \beta_p, \beta_u$  and  $y_s^*$  are defined as follows:

$$\beta = \eta R \sigma, \quad \beta_p = \eta(R - \omega_c), \quad \beta_u = \eta(R - \omega_u), \quad y_s^* = h - d = \frac{1.5}{\sqrt{108\pi\beta}}$$

$$\omega^* = z^* - d^*, \quad \omega_c^* = \omega_c / \sigma, \quad \omega_p^* = \omega^* - \omega_c^*, \quad \omega_{pu}^* = \omega^* - \omega_u^*,$$

In similar manner, the contact load may be written as;

$$P(d) = P_{e1}^* - P_{e2}^* + P_{p2}^* - P_{p3}^* \quad (22)$$

where the dimensionless contact load,  $P^*$ , is obtained by dividing the nominal contact pressure,  $P/A_n$ , by the hardness  $H$ , i.e.  $P^* = P/(A_n H)$ .

$$P_{e1}^*(d) = \frac{2}{3} \frac{\pi K \beta}{(\omega_c^*)^{0.5}} \int_{d+\omega_c}^{\infty} \omega^{3/2} \phi^*(d) dz \quad (23)$$

$$P_{e2}^*(d) = \frac{2}{3} \frac{\pi K \beta_p}{(\omega_c^*)^{0.5}} \int_{d+\omega_c}^{\infty} \omega_p^{3/2} \phi^*(d) dz \quad (24)$$

$$P_{p2}^*(d) = 2\pi K \beta_p \int_{d+\omega_c}^{\infty} \omega_p \phi^*(d) dz \quad (25)$$

$$P_{p3}^*(d) = 2\pi K \beta_u \int_{d+\omega_u}^{\infty} \omega_{pu}^* \phi(d) d z \quad (26)$$

## 7. Results and Discussions

For the purpose of comparing the results evaluated by KE (Kogut & Etsion, 2002), LL (Lin & Lin, 2005) models and the present model the equations established in these models and in the previous section are evaluated numerically. The area-separation and load-separation are investigated for typical values of plasticity index  $\Psi$ . The values of the plasticity index determine the nature of contact and are used to analyze the effect surface roughness and material properties on the contact of rough surfaces. For  $\Psi < 0.6$ , the contact is predominantly elastic and for  $\Psi > 1.0$ , the contact is predominantly plastic. Thus plasticity,  $\Psi$ , values are considered in the range of 0.5–2.5 in order to consider the whole range of deformation from predominantly elastic to predominantly plastic including elastic–plastic. The values of  $\beta$  are selected according to AF model (Abdo & Farhang, 2004) and the maximum contact pressure,  $K$ , are calculated from equations (14).

Fig. 5 (a) (b) (c) illustrates the dimensionless mean separation,  $h^*$ , vs. the dimensionless contact load,  $P^*$ , for various values of plasticity index  $\Psi$ . While the three models predict similar contact loads for low plasticity index,  $\Psi = 0.5$ , the present model predicts a lower values for materials of higher plasticity index.

Fig. 6 (a) (b) (c) depicts the dimensionless contact area vs. dimensionless separation for different values of plasticity index as predicted by KE, LL models and the present model. In the case of  $\Psi = 0.5$ , the total contact area curves of the three models almost grouped together over a wide range of dimensionless separations. If the plasticity index  $\Psi$  rises, the variations of the dimensionless total contact area for the three models are shown. The total contact load and area curves for plasticity index  $\Psi$  at 0.8 and 2.5 predicted by the present model are lower than the KE and LL curves. The variation came from the subtraction of the characteristic of contact corresponds to the contribution due to the elastic interference between the plane and the plastic asperity and the subtraction of the plastic portion of the interference that include the interference with the ultimate-stress asperity beyond expected failure. That is subtracting  $A_{e2}^*$  and  $A_{p3}^*$  integral forms to obtain the net contact area and subtracting  $P_{e2}^*$  and  $P_{p3}^*$  integral forms to obtain the net contact load. It is noteworthy to mention that in these integrals, the lower limit of the integration are shifted by apparent critical interferences  $\omega_c^*$  and  $\omega_u^*$ . Furthermore, the asperity curvature corresponding to plastic asperities as given in eqn. (4) and the asperity curvature corresponding to ultimate-stress asperity in eqn. (3) need to be used in the corresponding integrals in eqns. (21 and 26) and eqns. (19, 20, 24, and 25), respectively. Furthermore, when the plasticity index reaches 6, transition value of  $\Psi$  corresponds to  $\omega/\omega_c \cong 110$ , and beyond the three models predicts similar total contact area and load values and that the contact is approximately plastic.

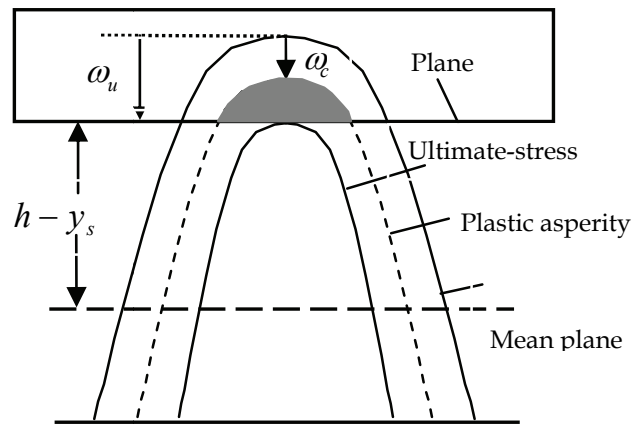


Fig. 3. Stages of interaction of flat surface on rough asperity

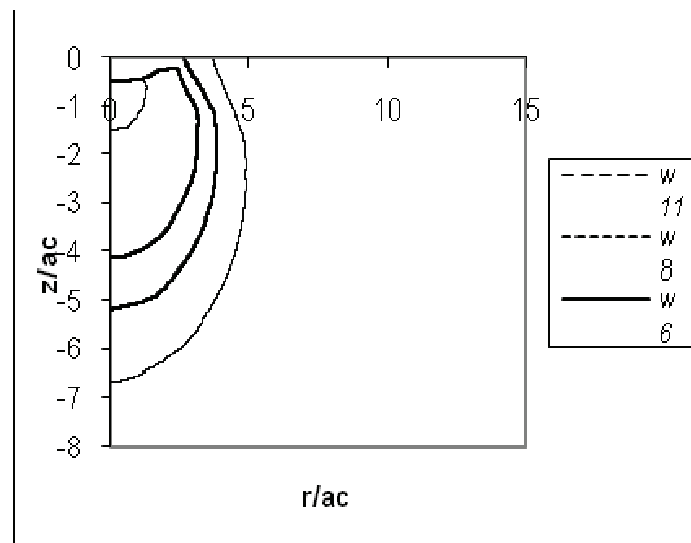
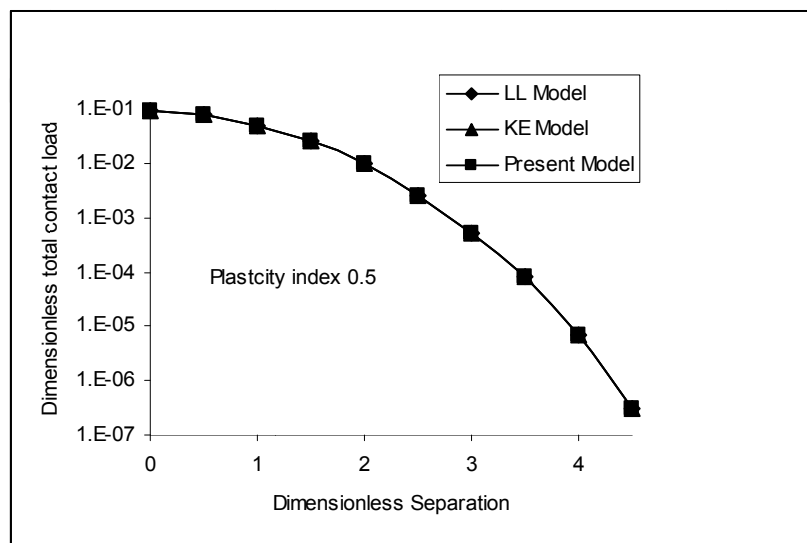
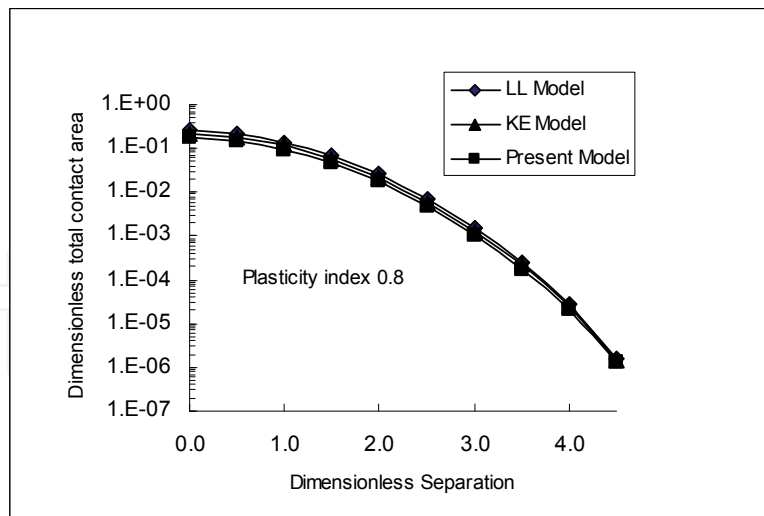


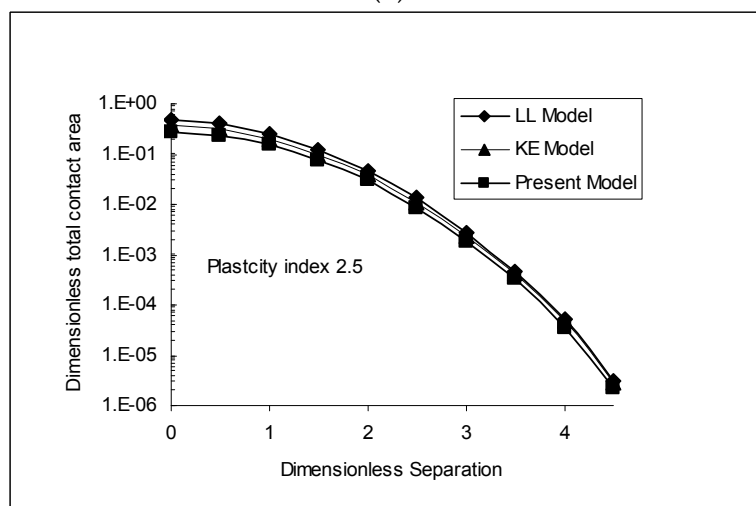
Fig. 4. Evolution of the plastic region in the asperity tip for a range (2-11) of  $\omega/\omega_c$



(a)

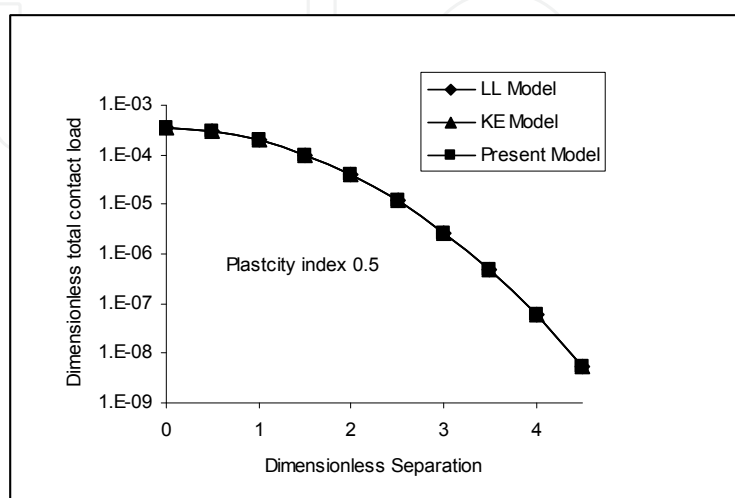


(b)

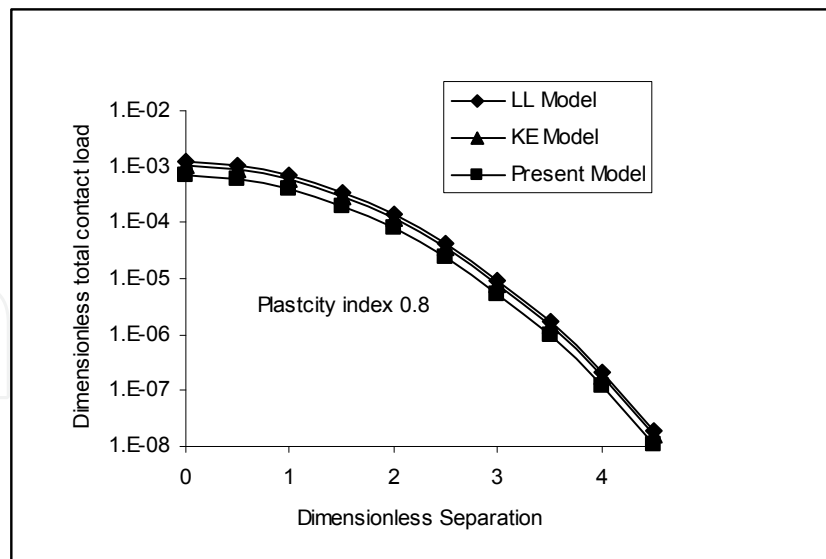


(c)

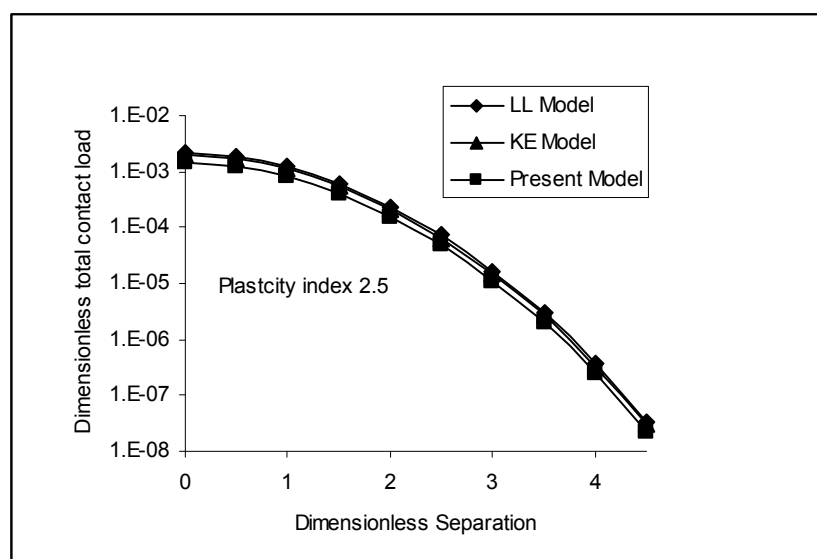
Fig. 5. Variation of the dimensionless total contact load with the dimensionless separation; (a)  $\Psi = 0.5$ , (b)  $\Psi = 0.8$ , (c)  $\Psi = 2.5$



(a)



(b)



(c)

Fig. 6. Variation of the dimensionless total contact area with the dimensionless separation; (a)  $\Psi = 0.5$ , (b)  $\Psi = 0.8$ , (c)  $\Psi = 2.5$

## 8. Conclusions

The contact area and contact load of an elastic-plastic micro-contact was calculated. The ultimate stress asperity is embedded at a critical depth within the actual surface asperities. The finite element solution is used to define the limit at which failure is to occur. The present model is more accurate than the previous models since it accounts for the net elastic-plastic by subtracting the plastic portion that reached the ultimate-stress asperity limit. Comparisons of the present model with the existing models for elastic-plastic contact have been performed. Results show that the previous elastic-plastic model underestimates the loading force particularly at elastic-plastic. Either total contact area or total contact load of

the rough surfaces depend is dependent upon the model developed for the elastic-plastic regime and the plasticity index. At a small plasticity index, these two contact parameters predicted by the three models are quite close. However, substantial differences in the contact parameters among these three models are apparent as the plasticity becomes sufficiently large. When the plasticity index reaches 6 and beyond the three models predicts similar total contact area and load values and that the contact is approximately plastic.

### Nomenclature

$Q$  = The characteristics of contact (area, or load),

$Q_{e1}$  = characteristic of contact corresponds to the contribution due to the elastic interference between the plane and surface asperity

$Q_{e2}$  = characteristic of contact corresponds to the contribution due to the elastic interference between the plane and plastic asperity

$Q_{p2}$  = contribution from plastic interaction due to the plastic interference of the plane and plastic asperity

$Q_{p3}$  = ultimate-stress asperity

$\omega_u$  = ultimate stress of the material

$R_p$  = radius of curvature of the plastic asperity

$R_u$  = radius of curvature for the ultimate-stress asperity

$R$  = radius of curvature for the original surface asperity

$Z$  = asperity height

$d$  = separation of the surfaces

$h$  = separation based on surface heights

$\sigma_s$  = Standard deviation corresponding to asperity

$\sigma$  = Standard deviation corresponding to Surface height

$y_s$  = The difference between  $h$  and  $d$

$N$  = total number of asperities

$\eta$  = density of asperities

$A_n$  = nominal area

$\omega^*$  = dimensionless interference

$A_e$  = elastic contact area

$P_e$  = elastic contact load

$A_p$  = plastic contact area

$P_p$  = plastic contact pressure

$H$  = hardness of the softer material of the contacting surfaces

$K$  = the hardness coefficient

$E$  = Hertz elastic modulus

$\nu$  = Poisson ratio of the softer material

$E_1, E_2$  = Young's moduli of the contacting surfaces

$\nu_1, \nu_2$  = Poisson's ratios of the contacting surfaces

$P_{\max}$  = maximum contact pressure

$P^*$  = dimensionless contact load

$\Psi$  = plasticity index

$h^*$  = dimensionless mean separation

## Appendix A

As illustrated in Fig. A.1, to obtain the mathematical description of the plastic asperity, the mapping of a point A on the surface to a point B on the plastic asperity must be considered. It is also noted that an asperity is described (Fig. A.1) in terms of a frame of reference whose origin is at the asperity peak and ordinate points towards the mean plane (Greenwood & Tripp, 1970). Therefore,  $\rho$ -y frame is used to describe the original asperity whereas  $xy$ -frame is employed for the plastic asperity.



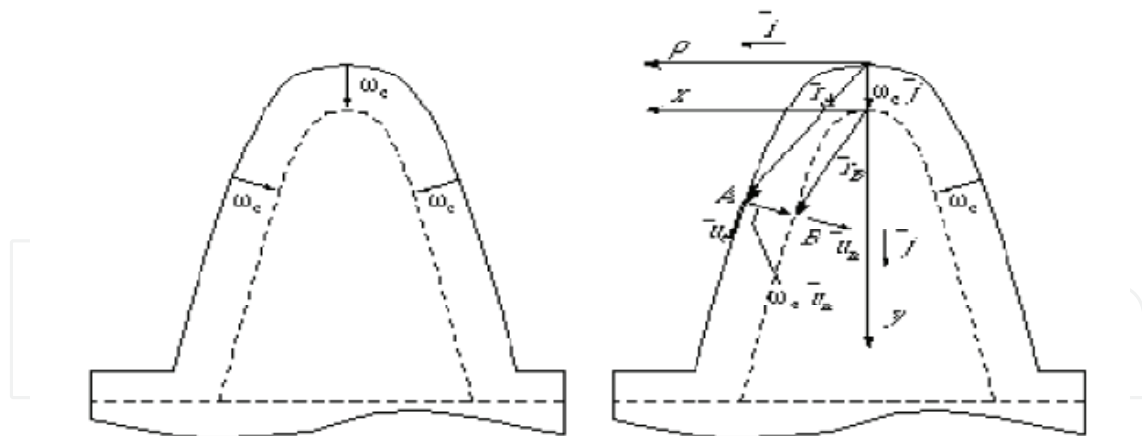


Fig A.1 - Plastic (fictitious) asperity shape

The respective positions of points A and B are denoted by  $\bar{r}_A$  and  $\bar{r}_B$ , as depicted in Fig. A.1. The position of point B on the fictitious asperity is

$$\bar{r}_B = -\omega_C \bar{j} + \bar{r}_A + \omega_C \bar{u}_n \quad (\text{A.1})$$

where,  $\bar{u}_n$  is the unit normal vector to the original asperity at point A. As usual the unit vectors  $\bar{i}$  and  $\bar{j}$  are defined along  $x$  and  $y$  axes, respectively. Employing the notation of Greenwood and Tripp

$$\bar{r}_A = \rho \bar{i} + \frac{1}{2R} \rho^2 \bar{j} \quad (\text{A.2})$$

Eqs. (A.1) and (A.2) may be used to obtain the equation describing the plastic asperity as follows:

Consider an asperity and assume that its shape is quadratic as proposed by Greenwood and Tripp. The equation of the surface asperity is given by

$$y = \frac{1}{2R} \rho^2 \quad (\text{A.3})$$

as shown in Fig. A.1. The figure also illustrates fictitious plastic asperity whose shape is obtained by a displacement of  $\omega_C$  along the normal to the quadratic curve. Let  $\bar{u}_t$  and  $\bar{u}_n$  represent the tangential and normal unit vector to the quadratic at point A. The position of point A is given by vector  $\bar{r}_A$  as

$$r_A = \rho \bar{i} + y \bar{j} = \rho \bar{i} + \frac{\rho^2}{2R} \bar{j} \quad (\text{A.4})$$

The unit tangential vector is obtained as

$$\bar{u}_t = \frac{d\bar{r}_A}{|d\bar{r}_A|} = \frac{1}{\sqrt{1 + \frac{\rho^2}{R^2}}} \left( \bar{i} + \frac{\rho}{R} \bar{j} \right) \quad (\text{A.5})$$

Hence the unit normal vector is:

$$\bar{u}_n = \frac{1}{\sqrt{1 + \frac{\rho^2}{R^2}}} \left( -\frac{\rho}{R} \bar{i} + \bar{j} \right) \quad (\text{A.6})$$

Then the description of the plastic asperity is obtained by

$$\bar{r}_B = \bar{r}_A + \omega_c \bar{u}_n - \omega_c \bar{j} \quad (\text{A.7})$$

Or

$$\bar{r}_B = \rho \left( 1 - \frac{\omega_c / R}{\sqrt{1 + \frac{\rho^2}{R^2}}} \right) \bar{i} + \left( \frac{\rho^2}{2R^2} + \frac{\omega_c}{\sqrt{1 + \frac{\rho^2}{R^2}}} - \omega_c \right) \bar{j} \quad (\text{A.7})$$

For small  $\omega_c / R$  and  $\rho / R$ ,  $\bar{r}_B$  maybe approximated by,

$$\bar{r}_B = \rho \left( 1 - \frac{\omega_c}{R} \right) \bar{i} + \frac{\rho^2}{2R} \left( 1 - \frac{\omega_c}{R} \right) \bar{j} \quad (\text{A.8})$$

Let

$$x = \rho \left( 1 - \frac{\omega_c}{R} \right)$$

Then

$$\bar{r}_B = x \bar{i} + \frac{x^2}{2(R - \omega_c)} \bar{j} \quad (\text{A.9})$$

Therefore the shape of the plastic asperity is given by:

$$y = \frac{x^2}{2(R - \omega_c)} \quad (\text{A.10})$$

Using the critical interference and additionally by imposing the conservation of volume, (Chang et al, 1986). derived the modified equations describing the contact area and load on an asperity:

$$A_0 = \frac{\pi a^2}{4} = \pi R \omega \left( 2 - \frac{\omega_c}{\omega} \right) \quad (\text{A.11})$$

And

$$P_0 = \pi R \omega \left( 2 - \frac{\omega_c}{\omega} \right) KH \quad (\text{A.12})$$

Since the plastic asperities only deform plastically, their introduction allows the reduction of equations (A.11) and (A.12) to the well known forms:

$$A_0 = 2\pi R_p \omega \quad (\text{A.13})$$

$$P_0 = 2\pi KHR_p \omega \quad (\text{A.14})$$

where,  $R_p$  represents the summit radius of curvature of the plastic asperity. Based on Eqn. (19), this radius of curvature is:

$$R_p = (R - \omega_c) \quad (\text{A.15})$$

## 9. References

- Abdo J. and AL-Yahmadi A. (2004), A wear model for rough surfaces based on the ultimate stress asperity concept *International Journal of Applied Mechanics and Engineering*, 9, pp. 11-19.
- Abdo J. and Farhang K. (2005), Elastic-plastic contact model for rough surfaces based on plastic asperity concept, *Int. J. Non-Linear Mech.*, 2005; 40(4), pp. 495
- Abdo J. (2006), Investigation of contact stiffness and its relation to friction-induced noise and vibration, *International Journal of Modeling and Simulation*; 26/4, pp. 295.
- Archard J. F. (1953), Contact and rubbing of flat surfaces. *J. Appl. Phys.* 24, pp. 981-988
- Brockley C. A. and Ko P. L. (1970), The measurement of friction and friction-induced vibration. *ASME J. Lubrication Technology* 92, 2007, pp. 543-549.

- Bush A.W., Gibson R.D., Thomas T.R. (1975), The elastic contact of a rough surface, *Wear*, V 35 (1975), pp. 87-111.
- Chang W.R., Etsion, I., and Bogy, D.B. (1986), Bogy, An elastic-plastic model for the contact of rough surfaces, *J. Tribol.* 109, (1986), pp. 257-263.
- Eid H., George G.A (2007), An elastic-plastic finite element analysis of interacting asperities in contact with a rigid flat, *J. Phys. D: Appl. Phys.* 40, 2007, 7432.
- Greenwood J.A., Williamson J.B.P. (1966), Contact of nominally flat surfaces, *Proc. Roy. Soc. (London)*, A 295 (1966), pp. 300-319.
- Greenwood J.A., Tripp J.H. (1967), The elastic contact of rough sphere, *ASME J. Appl. Mech.* 34 (1967), pp. 153-159.
- Greenwood, J. A., and Tripp, J. H (1970), The Contact of Two Rough Nominally Flat Rough Surfaces, *Proc. Instn. Mech. Engrs.*, V. 185, pp. 625-633.
- Halling J., Nuri K. A., Eds. De Pater and Kalker. (1975), The normal approach between rough flat surfaces in contact, *Wear*, Volume 32, Issue 1, pp. 81-93
- Hisakado T. (1974), Effect of surface roughness on contact between solid surfaces, *Wear*, V 28 (1974), pp. 217-234.
- Ibrahim, R. A. and Rivin, E. (1994-I), Friction-Induced Vibration, Chatter, Squeal, and Chaos; Part I: Mechanics of Contact and Friction; eds., *Applied Mechanics Reviews*, Vol. 47, 227, pp. 209-253.
- Ibrahim, R. A. and Rivin, E. (1994-II), Friction-Induced Vibration, Chatter, Squeal, and Chaos; Part II: Mechanics of Contact and Friction; eds., *Applied Mechanics Reviews*, Vol. 47, pp. 209-253.
- Ishigaki h., Kawaguchi I., Mizuta S. (1979), A simple estimation of the elastic-plastic deformation of contacting asperities, *Wear*, V 54 (1979), pp. 157-164.
- Jackson R.L., Green I., Quicksall J.J. (2004), Elasto-plastic hemispherical contact models for various mechanical properties, *Proc. Instn Mech. Engrs: J. Engineering Tribology*, Vol. 218 Part J, pp. 13-322.
- Karl, E. R., Komvopoulos, K., and Bogy, D. B. (1993), Elastic-Plastic Finite Element Analysis of Repeated Indentation of Half-Space by Rigid Sphere, *ASME J. Appl. Mech.*, 1993; 60, pp. 829.
- Kogut, L. and Etsion, I. (2002), A finite element based elastic-plastic model for the contact of rough surfaces *ASME Jour. of Appl. Mech.*, 2002; 69, pp. 657
- Kogut, L. and Etsion, I. (2003), A Finite Element Based Elastic-Plastic Model for the Contact of Rough Surfaces, *Trib. Trans.* 2003; 46, pp. 383-390.
- Kucharski, S., Klimczak, T., Polijaniuk, A. and Kaczmarek, J. (1994), Finite-elements model for the contact of rough surfaces, *Wear*, 1994; 177, 1.
- Lin L. and Lin J. (2005), An Elastoplastic Micro-asperity Contact Model for Metallic Materials, *ASME J. Tribol.*, 2005; 127, pp. 666
- Liu G. Zhu, J., Wang, Q. J. (2001), Elasto-Plastic Contact of Rough Surfaces, *Tribol. Trans.*, 44; 2001, pp. 437.
- McCool J.I. (1986), Predicting microfracture in ceramics via a microcontact model, *ASME J. Tribol.* 108 (1986), pp. 380-386.
- Mulhearn T. O. and Samuels L. E., The abrasion of metals: A model of the process, *wear*, Volume 5, Issue 6, November-December 1962, pp. 478-498
- Pullen, J., Williamson (1972), On the plastic contact of rough surfaces, *Proc. Roy. Soc. (London)*, A 327 (1972), pp.159-173.

- Samuels L. E. (1978), The mechanisms of abrasive machining, *AATA Number*: 16-905, Volume Number: 239, pp. 132-152.
- Tzou, k., Wickert, J., Akay, A (1998), In-plane vibration modes of arbitrarily thick disks. *ASME Journal of Vibration and Acoustics* **120** (1998a), pp. 384-391.
- Zhao, Y., Maietta, D. M., and Chang, L. (2000), An Asperity micro-contact model incorporating the transition from elastic deformation to fully plastic flow, *ASME J. Tribol.*, 2000; 122(1), pp. 86.

IntechOpen

IntechOpen



## **Finite Element Analysis**

Edited by David Moratal

ISBN 978-953-307-123-7

Hard cover, 688 pages

**Publisher** Sciyo

**Published online** 17, August, 2010

**Published in print edition** August, 2010

Finite element analysis is an engineering method for the numerical analysis of complex structures. This book provides a bird's eye view on this very broad matter through 27 original and innovative research studies exhibiting various investigation directions. Through its chapters the reader will have access to works related to Biomedical Engineering, Materials Engineering, Process Analysis and Civil Engineering. The text is addressed not only to researchers, but also to professional engineers, engineering lecturers and students seeking to gain a better understanding of where Finite Element Analysis stands today.

### **How to reference**

In order to correctly reference this scholarly work, feel free to copy and paste the following:

Jamil Abdo, Danish Haneef and Abdullah Al-Shabibi (2010). Finite Element Modelling of Elastic-Plastic Contact of Rough Surfaces, Finite Element Analysis, David Moratal (Ed.), ISBN: 978-953-307-123-7, InTech, Available from: <http://www.intechopen.com/books/finite-element-analysis/finite-element-modelling-of-elastic-plastic-contact-of-rough-surfaces>

**INTECH**  
open science | open minds

### **InTech Europe**

University Campus STeP Ri  
Slavka Krautzeka 83/A  
51000 Rijeka, Croatia  
Phone: +385 (51) 770 447  
Fax: +385 (51) 686 166  
[www.intechopen.com](http://www.intechopen.com)

### **InTech China**

Unit 405, Office Block, Hotel Equatorial Shanghai  
No.65, Yan An Road (West), Shanghai, 200040, China  
中国上海市延安西路65号上海国际贵都大饭店办公楼405单元  
Phone: +86-21-62489820  
Fax: +86-21-62489821

© 2010 The Author(s). Licensee IntechOpen. This chapter is distributed under the terms of the [Creative Commons Attribution-NonCommercial-ShareAlike-3.0 License](#), which permits use, distribution and reproduction for non-commercial purposes, provided the original is properly cited and derivative works building on this content are distributed under the same license.

IntechOpen

IntechOpen